Atmos. Chem. Phys., 13, 12187–12197, 2013
www.atmos-chem-phys.net/13/12187/2013/
doi:10.5194/acp-13-12187-2013

Atmospheric Chemistry and Physics Open Access

Net influence of an internally generated quasi-biennial oscillation on modelled stratospheric climate and chemistry

M. M. Hurwitz[1,2], **L. D. Oman**[2], **P. A. Newman**[2], **and I.-S. Song**[3]

[1]Goddard Earth Science Technology and Research (GESTAR), Morgan State University, Baltimore, MD, USA
[2]NASA Goddard Space Flight Center, Greenbelt, MD, USA
[3]Korea Institute of Atmospheric Prediction Systems (KIAPS), Seoul, South Korea

Correspondence to: M. M. Hurwitz (margaret.m.hurwitz@nasa.gov)

Received: 22 March 2013 – Published in Atmos. Chem. Phys. Discuss.: 23 May 2013
Revised: 12 August 2013 – Accepted: 6 November 2013 – Published: 17 December 2013

Abstract. A Goddard Earth Observing System Chemistry-Climate Model (GEOSCCM) simulation with strong tropical non-orographic gravity wave drag (GWD) is compared to an otherwise identical simulation with near-zero tropical non-orographic GWD. The GEOSCCM generates a quasi-biennial oscillation (QBO) zonal wind signal in response to a tropical peak in GWD that resembles the zonal and climatological mean precipitation field. The modelled QBO has a frequency and amplitude that closely resembles observations. As expected, the modelled QBO improves the simulation of tropical zonal winds and enhances tropical and subtropical stratospheric variability. Also, inclusion of the QBO slows the meridional overturning circulation, resulting in a generally older stratospheric mean age of air. Slowing of the overturning circulation, changes in stratospheric temperature and enhanced subtropical mixing all affect the annual mean distributions of ozone, methane and nitrous oxide. Furthermore, the modelled QBO enhances polar stratospheric variability in winter. Because tropical zonal winds are easterly in the simulation without a QBO, there is a relative increase in tropical zonal winds in the simulation with a QBO. Extratropical differences between the simulations with and without a QBO thus reflect the westerly shift in tropical zonal winds: a relative strengthening of the polar stratospheric jet, polar stratospheric cooling and a weak reduction in Arctic lower stratospheric ozone.

1 Introduction

The quasi-biennial oscillation (QBO) is the leading mode of variability in the tropical lower and middle stratosphere (Baldwin et al., 2001). The QBO is characterized by a downward-propagating pattern of alternating easterly and westerly zonal winds in the equatorial region, with a period of approximately 28 months, and is driven by both gravity and planetary-scale waves (Lindzen and Holton, 1968; Holton and Lindzen, 1972). The zonal wind QBO induces changes in the tropical stratospheric circulation, affecting the concentrations of ozone and other trace constituents (Gray et al., 1989; Butchart et al., 2003; Tian et al., 2006).

The phase of the QBO contributes to interannual variability in the polar stratosphere. Holton and Tan (1980) and Lu et al. (2008) showed that the phase of the QBO modulates the strength of the Arctic vortex in mid-winter; the vortex is weakest during the easterly phase of the QBO. QBO phase-related differences in the strength of the polar vortices modulate polar ozone loss (Lait, 1989; Randel and Cobb, 1994). Analogously to the Arctic response, the Antarctic vortex is generally weaker during the easterly phase of the QBO (Baldwin and Dunkerton, 1998). Also, the phase of the QBO modulates the polar stratospheric response to El Niño and La Niña events (Garfinkel and Hartmann, 2007; Hurwitz et al., 2011a). However, as the QBO signal is intrinsic to the observational record, the time-averaged impact of the easterly and westerly phases of the QBO on mean zonal wind, temperature and trace constituents is difficult to evaluate using atmospheric data.

A chemistry-climate model (CCM) is an ideal tool for understanding the net impact of the QBO. Punge and Giorgetta (2008) quantified the net effect of the QBO on the late 20th century stratospheric climate by comparing two CCM simulations: one without a QBO signal, and the other with zonal winds between 90 hPa and 10 hPa nudged to profiles taken at Singapore. The authors found that inclusion of this QBO signal impacted stratospheric zonal winds, temperature and ozone, mainly in the deep tropics. The vertical pattern of changes in tropical upwelling was consistent with changes in the distribution of trace species. However, the value of the conclusions reached by Punge and Giorgetta (2008) may be limited because the authors tested a "nudged" (i.e. prescribed) QBO. Nudging to observed zonal winds does not allow the tropical and mid-latitude stratosphere to adjust internally to changes in, for example, the QBO phase, nor does it allow for full interaction between stratospheric ozone and climate.

The Goddard Earth Observing System Chemistry-Climate Model (GEOSCCM) version 2 can be run with or without an internally generated QBO. In the formulation of the GEOSCCM evaluated by SPARC CCMVal (2010), both tropical lower stratospheric variability and the QBO amplitude were negligible. In contrast, a more recent model formulation (introduced by Hurwitz et al., 2011b) can internally generate a QBO with a realistic periodicity and amplitude, depending on the latitudinal structure of the non-orographic gravity wave drag (GWD). Comparing two simulations using this formulation of the GEOSCCM, one with a QBO and another without, this paper quantifies the net effect of the modelled QBO on stratospheric climate and variability. Section 2 provides a brief description of the GEOSCCM, as well as the two above-mentioned simulations. The net effects of the modelled QBO on the mean and variance of stratospheric zonal winds, temperature, mean age, stratospheric circulation, ozone, nitrous oxide and methane are shown in Sect. 3. Section 4 provides a summary and brief discussion.

2 Model and simulations

This paper considers the net impact of the QBO in version 2 of the GEOSCCM. The GEOSCCM couples the GEOS-5 general circulation model (Molod et al., 2012) with a comprehensive stratospheric chemistry module (Pawson et al., 2008). The GEOSCCM performed well in the SPARC CCMVal (2010) detailed evaluation of stratospheric processes. The present formulation of the GEOSCCM is the same as in Hurwitz et al. (2011b). In this formulation, the model has 2° latitude × 2.5° longitude horizontal resolution and 72 vertical layers, with a model top at 0.01 hPa. Predicted distributions of water vapour, ozone, methane, nitrous oxide, CFC-11, CFC-12 and HCFC-22 feed back to the radiative calculations.

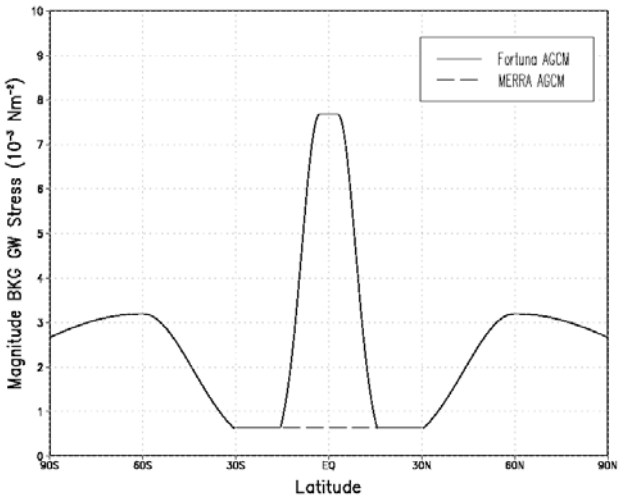

Fig. 1. Background non-orographic gravity wave drag in the *Q* simulation (shown as the solid black line) and *N* simulation (shown as the dashed black line). Reproduced with permission from Molod et al. (2012).

In the GEOSCCM, tropical stratospheric zonal wind variability depends on the details of the non-orographic GWD scheme. As the generation of non-orographic gravity waves often accompanies precipitation (e.g. convective and frontal systems; see Richter et al. (2010)), the latitudinal structure of the gravity wave spectrum is designed to mimic the structure of the climatological mean precipitation field (solid black line in Fig. 1; reproduced with permission from Molod et al., 2012). A 700 km wavelength is used for the tropical non-orographic waves to prevent an excessive downward propagation of the semi-annual oscillation into the lower stratosphere, and thus contamination of the QBO signal. With a tropical peak in non-orographic gravity wave stress, the present model formulation generates a QBO signal in equatorial zonal winds (see Sect. 3.1). Prior to this model formulation, the GEOSCCM did not generate a QBO: zonal winds in the equatorial lower stratosphere were generally easterly (see Fig. 2e and SPARC CCMVal, 2010).

Two GEOSCCM simulations are used to assess the net stratospheric impacts of the QBO. The two simulations are identical, except for the magnitude of the non-orographic GWD stress applied in the deep tropics. The first simulation (hereafter "*Q*") has a strong peak in tropical GWD, which as described above, generates a QBO signal. The second simulation (hereafter "*N*") has weak tropical GWD stress (dashed black line in Fig. 1), and thus does not have a QBO.

Both simulations are 50 yr "time-slice" simulations with fixed climate forcings and annually repeating sea surface temperature (SST) and sea ice climatologies. Surface mixing ratios of the primary greenhouse gases and ozone-depleting substances are specified from 2005 concentrations. The SST and sea ice climatologies are composites of 10 El

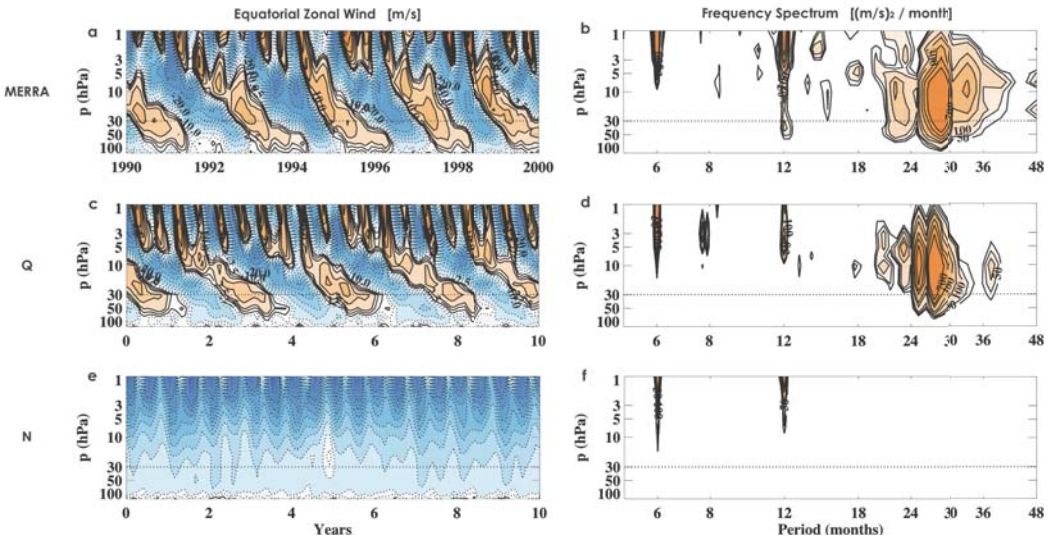

Fig. 2. Equatorial (4° S–4° N) zonal wind (m s^{-1}) in **(a–b)** MERRA reanalysis, 1979–2012, **(c–d)** the *Q* simulation, and **(e–f)** the *N* simulation. **(a, c, e)** 10 yr time series, **(b, d, f)** frequency spectra for the entire span of the MERRA reanalysis and GEOSCCM simulations. Black dotted lines indicate the 30 hPa level.

Niño–Southern Oscillation (ENSO)-neutral years that span the satellite era (as in Hurwitz et al., 2011b). HadISST1 SSTs and sea ice concentrations at 1° × 1° resolution (Rayner et al., 2003) are used to prepare the composites. Variability related to the solar cycle and volcanic eruptions is not considered.

Modelled temperature and zonal wind fields are compared with the Modern Era Retrospective-Analysis for Research and Applications (MERRA). MERRA is a meteorological reanalysis, based on an extensive set of satellite observations and on the Goddard Earth Observing System Data Analysis System, version 5 (GEOS-5), from 1979 through the present (Rienecker et al., 2011). The MERRA reanalysis has vertical coverage up to 0.1 hPa and, for this study, is interpolated to 1.25° × 1.25° horizontal resolution.

Additionally, simulated stratospheric mean age of air, ozone, nitrous oxide and methane are compared with observational data sets. Simulated mean age of air is compared with profiles derived from CO_2 and SF_6 observations (Andrews et al., 2001; Engel et al., 2009). These observations were taken between 1986 and 2005. Simulated ozone (O_3) and nitrous oxide (N_2O) are compared with the 2004–2012 climatology of the Aura Microwave Limb Sounder (MLS) version 3.3 O_3 and N_2O products (Froidevaux et al., 2008; Jiang et al., 2007; Livesey et al., 2008, 2011). Simulated methane (CH_4) is compared with the UARS HALOE climatology for 1991–2002 (Russell et al., 1993; Grooss et al., 2005). The UARS HALOE climatology is scaled by 1.02 to reflect the increase in methane surface mixing ratio between the mid-1990s and 2005 (see http://www.esrl.noaa.gov). More details about each data set are provided in Sect. 1 of SPARC CCMVal (2010).

3 Results

3.1 Equatorial zonal winds

The QBO in zonal winds is well simulated in *Q*. The left-hand panels of Fig. 2 show 10 yr time series of equatorial winds in the MERRA reanalysis (1990–1999; Fig. 2a), *Q* (Fig. 2c) and *N* (Fig. 2e). The right-hand panels of Fig. 2 show the frequency spectra for equatorial winds for 1979–2012 in MERRA (Fig. 2b) and for the entire *Q* and *N* simulations (Fig. 2d and f). The simulated QBO signal has realistic amplitude and periodicity (compare Fig. 2a and c). In *Q*, the simulated peak frequency is 27 months at 30 hPa (Fig. 2d), with a secondary peak at 25 months, compared with 28 months in the MERRA reanalysis (Fig. 2b). In the upper and middle stratosphere, the annual (12-month) and semi-annual (6-month) frequencies are well simulated. The annual frequency is weaker than observed in the lower stratosphere. Note that the simulated QBO signal is weaker than observed below 50 hPa (Hurwitz et al., 2011b).

Equatorial zonal winds are easterly throughout the *N* simulation, without a QBO signal (Fig. 2e). That is, lower stratospheric zonal wind variability is negligible. However, the annual and semi-annual frequencies are simulated in the middle and upper stratosphere (Fig. 2f).

3.2 Annual mean impact of the QBO

Inclusion of the QBO impacts stratospheric mean climate and variability. Figures 3, 5 and 6 show the 50 yr annual mean zonal wind, temperature, age of air, residual vertical and meridional velocities, methane, nitrous oxide and ozone fields in the *N* simulation (left-hand panels), *Q* simulation

(middle panels) and differences between Q and N (i.e. the net mean impact of the QBO) (right-hand panels). Figure 4 shows QBO-related changes in stratospheric variability for each field. Annual and zonal mean zonal winds in the Q simulation are easterly in the tropical stratosphere and westerly in the extratropics (Fig. 3b), in good agreement with the MERRA reanalysis (black contours). In N, tropical stratospheric easterlies are on average stronger than in the MERRA reanalysis (Fig. 3a); thus, inclusion of the QBO represents both a relative zonal wind increase in the tropics (10–20 m s^{-1}) and an improvement in the simulated mean comparison with MERRA (compare Fig. 3a and b). As expected, zonal wind variability increases by 3–5 times in Q, as compared with N, throughout the tropical stratosphere (Fig. 4a).

The modelled stratospheric temperatures generally agree well with MERRA (Fig. 3d and e). A modest cold bias around 60° S may reflect the overly strong polar jet and delayed breakup of the Antarctic vortex in austral spring (Hurwitz et al., 2010). Inclusion of the QBO warms the tropical stratosphere and Arctic lower stratosphere, but cools the high-latitude upper stratosphere by $\sim$ 1 K (Fig. 3f). These temperature changes reflect a slowing of the stratospheric overturning circulation, as discussed below. QBO-related increases in temperature variability maximize in the middle stratosphere, in the deep tropics, with an additional lobe of increased variability around 30° S (Fig. 4b).

Inclusion of the QBO acts to slow the stratospheric circulation. Age of air is an indicator of the strength and structure of the meridional overturning (i.e. Brewer–Dobson) circulation (SPARC CCMVal, 2010). In the GEOSCCM, mean age is an inert tracer that measures the time since a parcel of air has left the troposphere. Because most air enters the stratosphere in the tropics, mean age values are lowest in the tropical lower stratosphere and highest in the high-latitude upper and middle stratosphere (Fig. 5a and b). $Q - N$ differences in annual mean age are generally positive throughout the stratosphere i.e., the QBO slows the overturning circulation (Fig. 5c). The largest increases in mean age ($\sim$ 0.3 yr) are seen in the tropical stratosphere around 10 hPa. Figure 7 shows observed and simulated mean age-of-air profiles in the deep tropics. While the mean age in N falls within the observational error, the older tropical mean age in the Q simulation is in better agreement with CO_2 and SF_6 observations. QBO-related changes in mean age variability, similarly to temperature variability, peak in the Southern Hemisphere tropical middle stratosphere (Fig. 4c). Decreased mean age in the lower stratosphere is consistent with slowing of the overturning circulation: less older air is advected downward into the mid-latitudes.

QBO-related changes in the residual circulation are consistent with the changes in mean age of air. In the upper stratosphere and polar regions, the net impact of the QBO is dominated by the slowing of the meridional circulation. At and above 10 hPa, $Q - N$ differences in $w*$ (residual vertical velocity) oppose the $w*$ climatology: negative differences in the tropics (weakened upwelling), and positive differences in the extratropics (weakened downwelling; compare Fig. 5e and f). In Fig. 5g–i, positive $v*$ (residual meridional velocity) values indicate poleward motion in both hemispheres. Negative differences in $v*$ (e.g. around 3 hPa) in the tropics and in the uppermost polar stratosphere reflect weakened poleward transport (Fig. 5i). In the lower and middle stratosphere, the net impact of the QBO is to enhance poleward transport. Positive $v*$ between 10 and 70 hPa, in the tropics and mid-latitudes, is consistent with enhanced mixing in this region. Note that the $v*$ differences are largest in the Southern Hemisphere and coincident with the peak change in $v*$ variability (Fig. 4e). Below 70 hPa, tropical $v*$ changes are positive. This set of $v*$ changes is consistent with the narrowing but strengthening of upward transport in the tropical lower stratosphere (Fig. 5f).

Both slowing of the stratospheric overturning circulation and enhanced lower stratospheric mixing affect the distribution of methane. Since methane is mainly transported into the stratosphere in the deep tropics, the distribution of stratospheric methane is inverted as compared with mean age: the highest concentrations are found in the tropical lower stratosphere, while the lowest values are found in the polar upper stratosphere. The structure of the simulated tropical and subtropical methane distribution matches the scaled UARS HALOE climatology, but with a high bias (Fig. 6a and b). This bias results from the stronger than observed transport in the GEOSCCM (SPARC CCMVal, 2010). Inclusion of the QBO decreases tropical and upper stratospheric methane mixing ratios, reflecting slowing of the stratospheric circulation (Fig. 6c). Given the negative latitudinal gradient in methane concentrations (Fig. 6b), increased lower stratospheric methane suggests enhanced meridional mixing (i.e. weakening of the subtropical transport barrier); this effect is further discussed below. Inclusion of the QBO generally increases methane variability, with the largest increases in the tropics and subtropical Southern Hemisphere (Fig. 4f).

QBO-related changes in N_2O provide further evidence for enhanced subtropical mixing. Similarly to methane, the highest N_2O concentrations are found in the tropical lower stratosphere, while the lowest values are found in the upper stratosphere (Fig. 6d and e). The simulated N_2O distribution matches the MLS climatology, but with a high bias in the tropical lower stratosphere, similar to the methane bias. Inclusion of the QBO weakens the meridional gradient of N_2O: decreasing equatorial N_2O (exceeding 30 ppbv) and increasing N_2O at subtropical latitudes (up to 10 ppbv) (Fig. 6f). Figure 8 shows the annual cycle of $Q - N$ differences in the subtropical N_2O gradient. Mean N_2O differences between 10 and 40° latitude serve as a proxy for the strength of the subtropical gradient (i.e. the strength of the subtropical mixing barrier). Negative differences indicate a weakening of the subtropical N_2O gradient, due to enhanced mixing (Douglass et al., 1999). The largest changes in subtropical N_2O

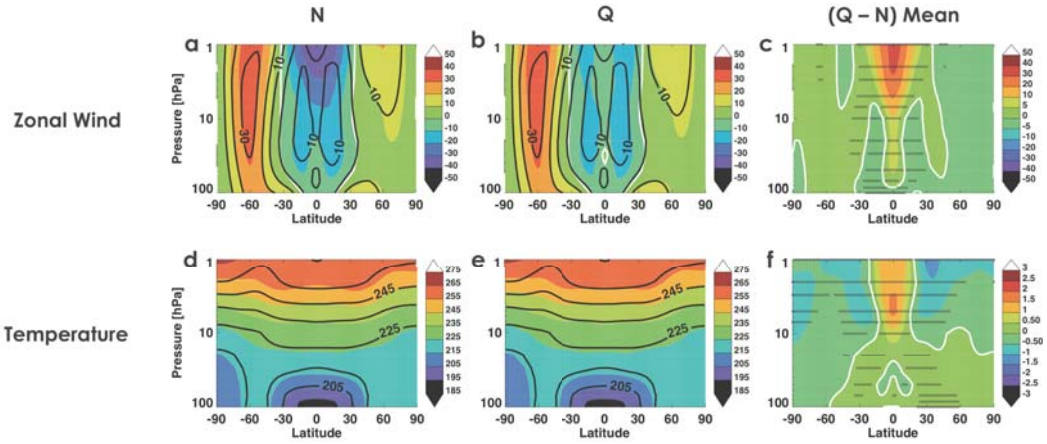

Fig. 3. (a–c) Zonal wind ($m\,s^{-1}$) and **(d–f)** temperature (K), for **(a, d)** N simulation zonal and annual mean and **(b, e)** Q simulation zonal and annual mean; black contours indicate MERRA reanalysis mean for 2000–2010. **(c, f)** $Q - N$ mean differences; white contours indicate zero difference; black Xs indicate changes significant at the 95 % level in a two-trailed t test.

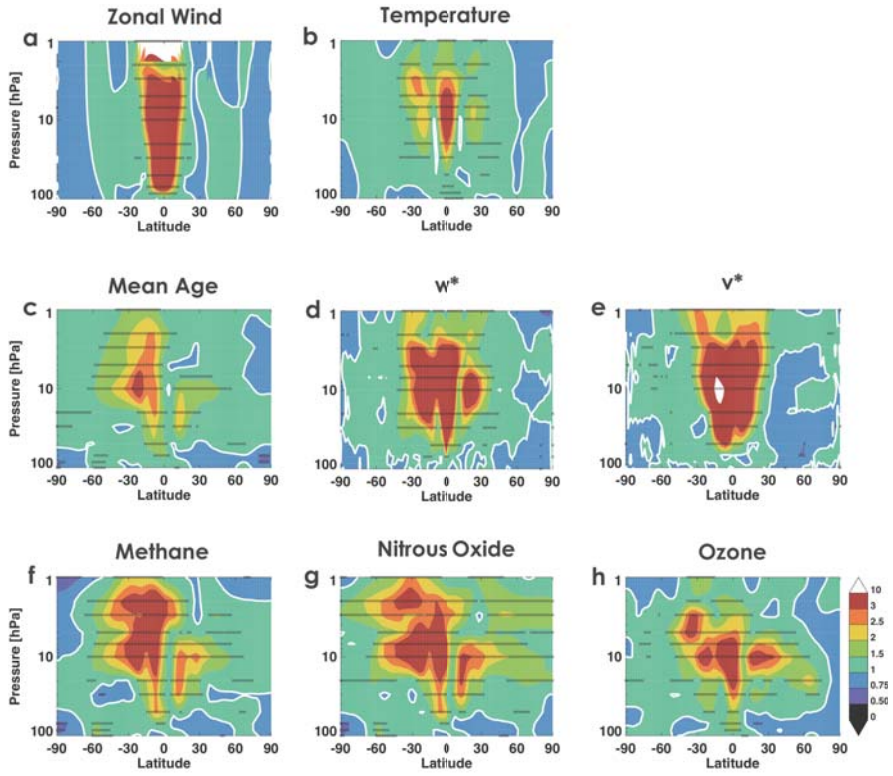

Fig. 4. Q/N changes in variance. White contours indicate where the variance ratio is equal to one. Black Xs indicate changes significant at the 95 % level in an f test.

are centred around 10 hPa (consistent with the increases in subtropical $v*$ and methane), in winter months. The QBO has a larger impact on subtropical N_2O in the SH (Fig. 8a) than in the NH (Fig. 8b), consistent with the relatively larger enhancements in variability in the SH (Fig. 4).

The net impact of the QBO on ozone reflects warming of the tropical stratosphere, enhanced subtropical mixing and slowing of the stratospheric overturning circulation. The annual mean ozone mixing ratio maximizes at approximately 10 ppmv in the deep tropics, at 10 hPa, and decreases with latitude (Fig. 6g and h). Simulated ozone

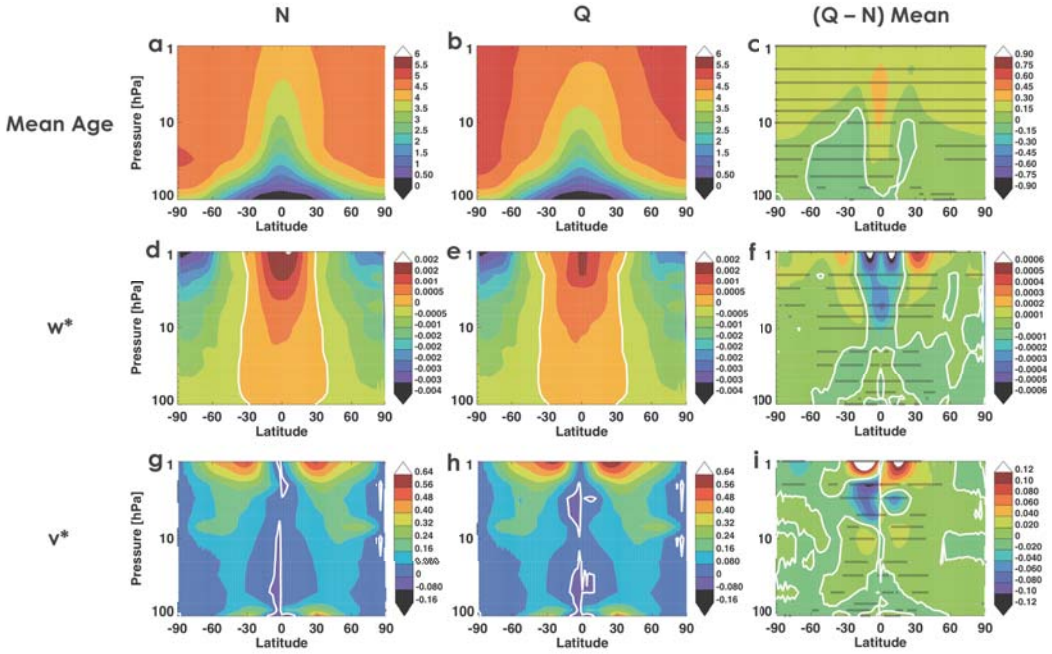

Fig. 5. As for Fig. 3, but for **(a–c)** mean age (years), **(d–f)** $w*$ (m s^{-1}) and **(g–i)** $v*$ (m s^{-1}). Note that values of $v*$ in the Southern Hemisphere are multiplied by -1, such that positive $v*$ values indicate poleward motion in both hemispheres.

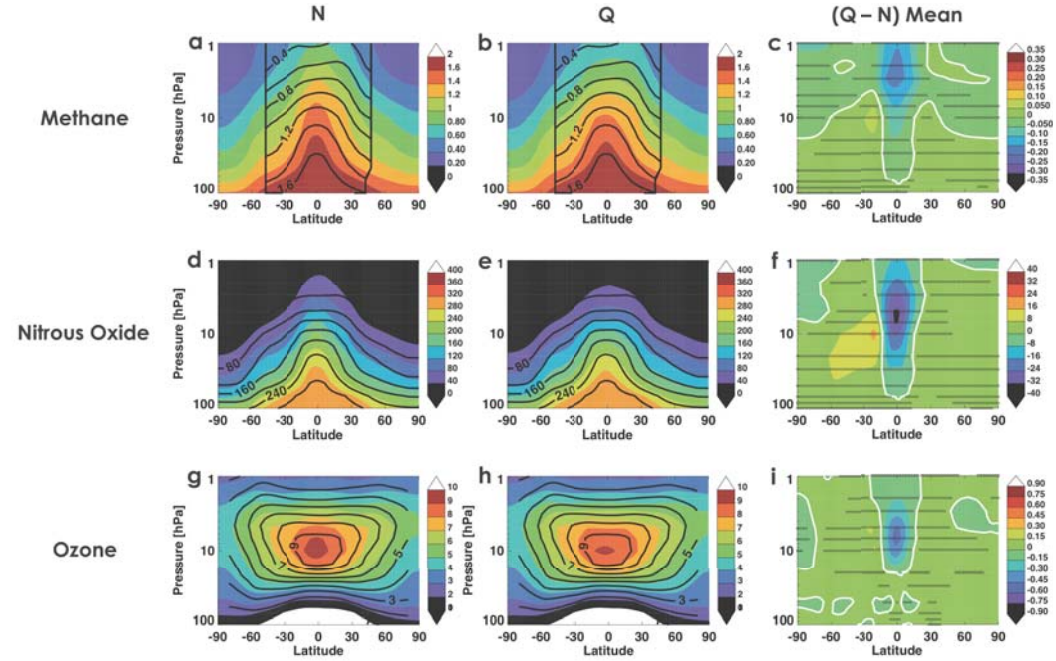

Fig. 6. As for Fig. 3, but for **(a–c)** methane (ppmv), **(d–f)** nitrous oxide (ppbv) and **(g–i)** ozone (ppmv). Black contours in **(a)** and **(b)** indicate the scaled HALOE climatology; black contours in **(d–e)** and **(g–h)** indicate MLS climatologies of nitrous oxide and ozone.

in the *Q* simulation is generally in agreement with the MLS ozone climatology (Fig. 6h). Thus, inclusion of the QBO improves model performance; the peak in ozone mixing ratio around 10 hPa is $\sim$0.8 ppmv too high in the *N* simulation. Relative warming of the tropical middle stratosphere in *Q* contributes to the negative ozone differences in the deep tropics (Figs. 3f and 6i). However, at the Equator at 10 hPa, the ratio between temperature and

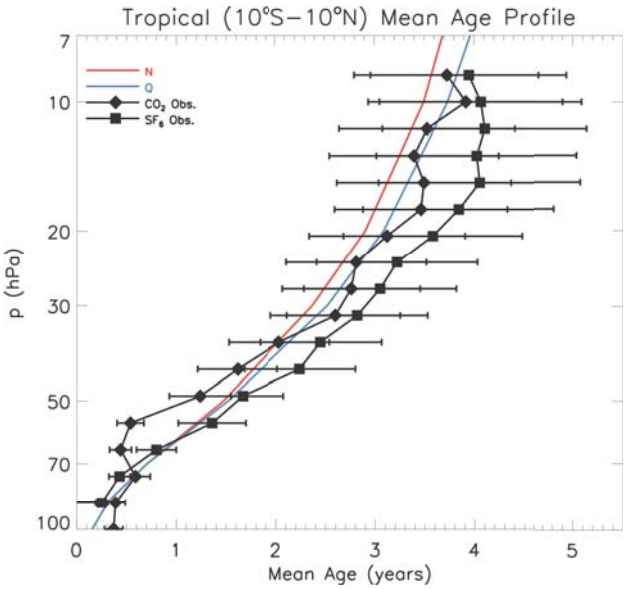

Fig. 7. Equatorial (10° S–10° N) mean age-of-air (years) profiles in the N simulation (red), Q simulation (blue), and from CO_2 (black diamonds) and SF_6 (black squares) observations.

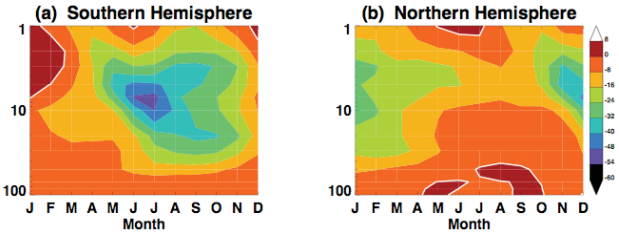

Fig. 8. $Q-N$ differences in the subtropical N_2O gradient (ppbv), as a function of month and altitude in **(a)** the Southern Hemisphere and **(b)** the Northern Hemisphere. Negative differences indicate weakening of the subtropical mixing barrier (i.e. enhanced subtropical mixing). White contours indicate zero differences.

ozone differences (i.e. $\Delta T / \Delta O_3 = 0.72\,K/0.8\,ppmv = 0.9$) does not agree with the ratio of ~ 6.7 as determined by Oman et al. (2010). This result suggests that other mechanisms contribute to the change in tropical ozone. Decreased tropical ozone at 10 hPa is consistent with both (1) strengthening of vertical upwelling below 10 hPa (Fig. 5f) and (2) enhanced mixing with mid-latitude air with relatively lower ozone concentrations (Fig. 6h and i).

3.3 High-latitude impact of the QBO in winter

In certain months, in the Q simulation, equatorial zonal winds are positively correlated with zonal winds in the polar stratosphere. That is, the GEOSCCM reproduces the Holton-Tan (1980) relation between the phase of the QBO and polar vortex strength: in winter, the polar vortices are

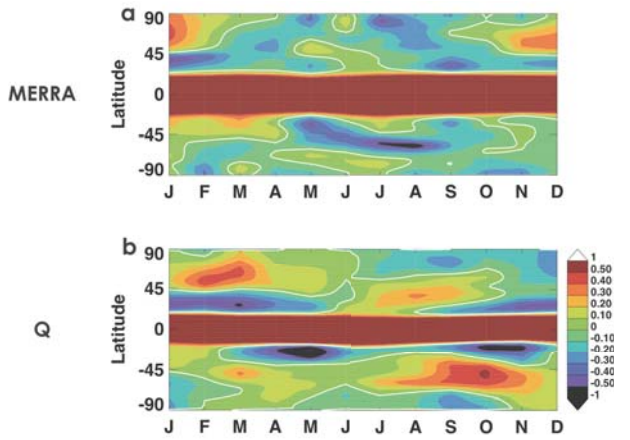

Fig. 9. 50 hPa zonal wind correlation with equatorial zonal winds, as a function of month and latitude, in **(a)** MERRA and **(b)** the Q simulation. White contours indicate zero correlation.

relatively stronger during the westerly phase of the QBO in the MERRA reanalysis (Fig. 9a). Figure 9b shows that, in the GEOSCCM, equatorial zonal wind correlations with zonal winds at 60° S are strong in, for example, September (Fig. 10), and at 60° N in January (Fig. 12).

The net impact of the QBO on zonal winds and temperature (i.e. $Q-N$) mimics the differences between the westerly and easterly phases of the QBO (i.e. in the Q simulation), at Southern Hemisphere high latitudes in September. Inclusion of the QBO strengthens the Antarctic jet (around 60° S) by 5–10 m s^{-1} (Fig. 10a). An equal strengthening is seen in Fig. 10b, which shows the zonal wind differences between the five Septembers in Q with the highest (i.e. QBO-W) equatorial zonal wind values at 30 hPa and the five Septembers in Q with the lowest (i.e. QBO-E) equatorial zonal wind values at 30 hPa. Note that the QBO-W − QBO-E differences are generally not statistically significant in the extratropics, due to the small size of the QBO-W and QBO-E composites.

Extratropical stratospheric temperatures decrease in September, consistent with the stronger zonal winds (i.e. by the thermal wind relation). Temperature differences are negative poleward of 45° S, both for $Q-N$ and QBO-W − QBO-E, with peak differences of 5 K in the Antarctic (Fig. 10c and d). Tropical and mid-latitude $Q-N$ differences reflect changes in stratospheric circulation and mixing (see Sect. 3.2).

Strengthening and cooling of the Antarctic polar vortex in September reflects the relative shift toward westerly tropical zonal winds, shifting the zero-wind line equatorward and decreasing planetary wave breaking at high latitudes. The magnitude of eddy heat flux at 40–80° S and 100 hPa diagnoses tropospheric planetary wave driving (Newman et al., 2001). The red line in Fig. 11 shows that eddy heat flux is reduced in the Q simulation relative to the N simulation, in August

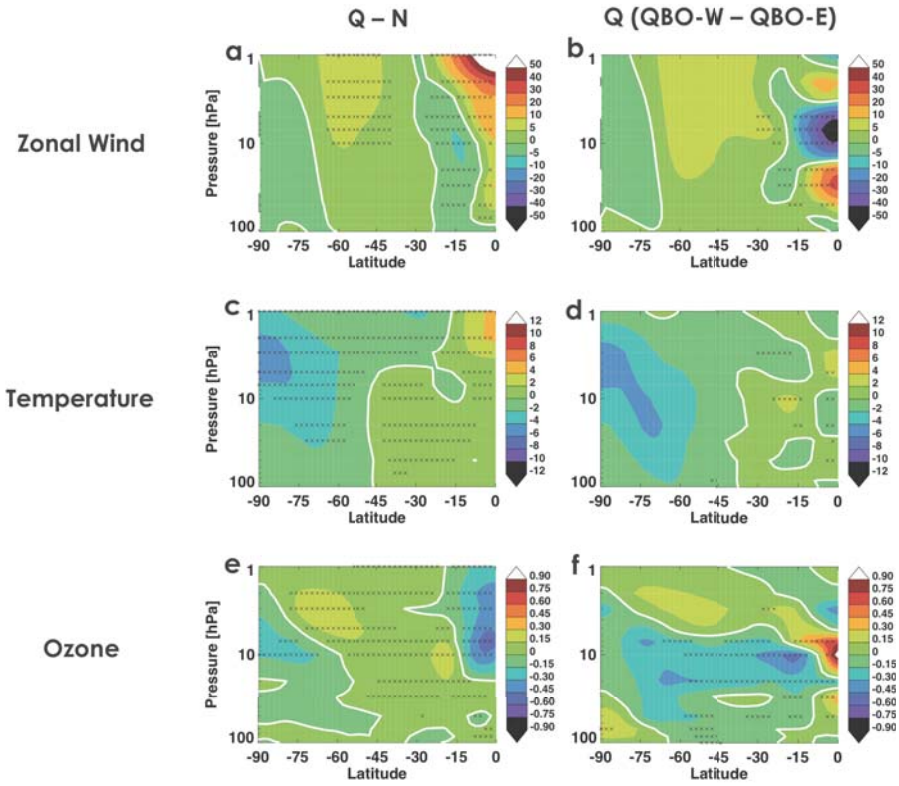

Fig. 10. September **(a–b)** zonal wind (m s^{-1}), **(c–d)** temperature (K) and **(e–f)** ozone (ppmv) differences in the Southern Hemisphere. **(a, c, e)** $Q - N$ mean differences; **(b, d, f)** QBO-westerly − QBO-easterly differences in the Q simulation. White contours indicate zero difference. Black Xs indicate differences significant at the 95 % level in a two-trailed t test.

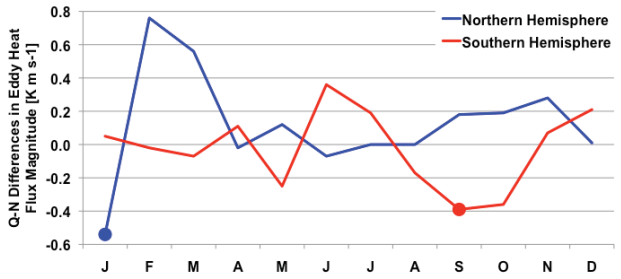

Fig. 11. $Q - N$ differences in eddy heat flux magnitude at 40°–80° latitude, 100 hPa in the Northern Hemisphere (blue line) and Southern Hemisphere (red line). Negative differences indicate a relative reduction in tropospheric planetary wave driving. The case shown in Fig. 10 is highlighted by the red circle. The case shown in Fig. 12 is highlighted by the blue circle.

through October. Note that the annual mean eddy heat flux difference is negligible.

Equivalent zonal wind and temperature differences are seen in the Northern Hemisphere extratropics in January. $Q - N$ differences reflect a relative shift toward the westerly phase of the QBO: a relative strengthening of the Arctic stratospheric jet (Fig. 12a and b) and cooling throughout the extratropical stratosphere (Fig. 12c and d). In this case, zonal wind and temperature differences are larger in response to QBO phase as compared with the net impact of the QBO. Strengthening and cooling of the Arctic vortex is caused by a dramatic reduction in planetary wave driving in January (Fig. 11, blue dot). Negative ozone differences in the Arctic lower stratosphere (Fig. 12e and f), though weak, hint at enhanced chemical ozone depletion, due to the cooler and more isolated polar air mass in January. The small size of the QBO-W and QBO-E composites likely weakens the statistical significance of the ozone differences.

4 Discussion

Inclusion of the QBO in a chemistry-climate model makes a significant difference to the mean stratospheric climate and variability. As expected, the addition of a QBO significantly enhances tropical variability. Extratropical zonal wind and temperature variability in winter is also enhanced. While the QBO is by definition an oscillating phenomenon, the multi-decadal mean of the modelled QBO modifies the mean climate. In particular, the following can be concluded:

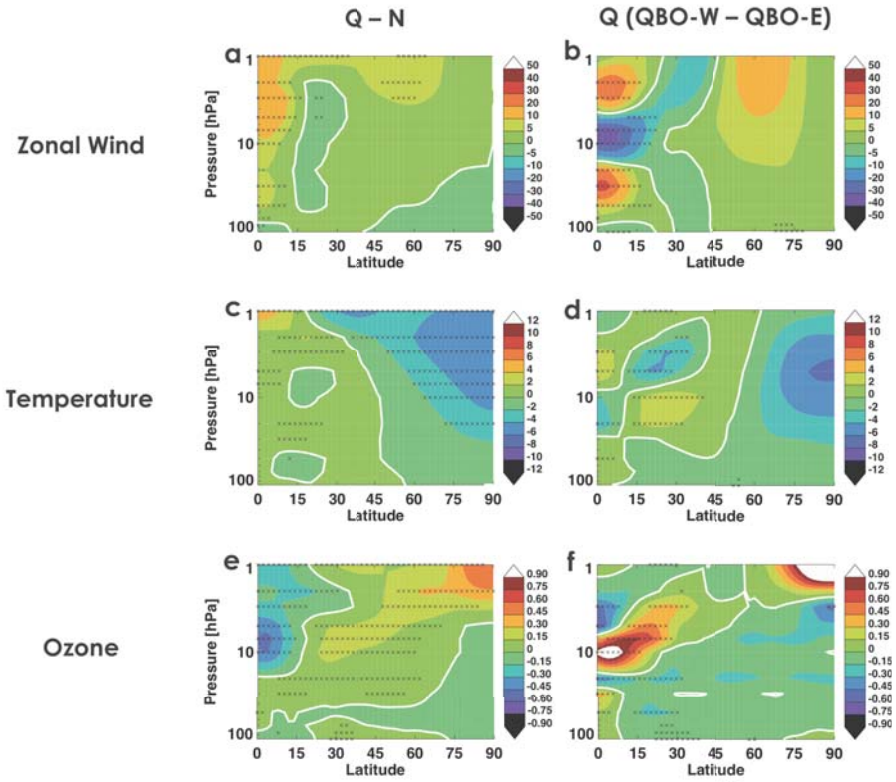

Fig. 12. January **(a–b)** zonal wind ($m\,s^{-1}$), **(c–d)** temperature (K) and **(e–f)** ozone (ppmv) differences in the Northern Hemisphere. **(a, c, e)** $Q - N$ mean differences; **(b, d, f)** QBO-westerly − QBO-easterly differences in the Q simulation. White contours indicate zero difference. Black Xs indicate differences significant at the 95 % level in a two-trailed t test.

1. *Addition of a QBO signal affects the mean stratospheric climate*. In the GEOSCCM, inclusion of a QBO signal slows the meridional overturning circulation, leading to older mean age of air throughout the stratosphere and affecting the distribution of trace species such as ozone, methane and nitrous oxide. The subtropical mixing barrier is weakened, enhancing methane and nitrous oxide in the extratropical lower stratosphere, and contributing to the reduced peak ozone mixing ratio at 10 hPa. The polar vortices are strengthened, particularly in winter. The net dynamical and transport impacts of the QBO generally improve model performance.

2. *The net impact of the QBO depends on both the baseline zonal wind field and the relative change in tropical zonal winds.* In the GEOSCCM, the baseline tropical zonal winds are easterly. In the simulation with a QBO signal, there is thus a relative increase in zonal winds in the tropical lower and middle stratosphere. Extratropical differences between simulations with and without a QBO reflect this shift toward the westerly zonal winds in the tropical stratosphere: a relative cooling and strengthening of the polar vortices, and a weak reduction in Arctic lower stratospheric ozone. The annual mean impact of the QBO on the polar stratosphere is larger in the GEOSCCM (up to $12\,m\,s^{-1}$, in both hemispheres) than in the MAECHAM4-CHEM CCM (no significant zonal wind differences) (Punge and Giorgetta, 2008), likely reflecting larger tropical zonal wind differences between the QBO and "no QBO" GEOSCCM simulations and/or increased statistical robustness due to the relatively greater length of the GEOSCCM simulations.

The QBO has a robust net impact on the mean stratospheric climate and trace gas distributions. In the case of the GEOSCCM, inclusion of the QBO yields better agreement between the simulated fields and climatological averages derived from a meteorological reanalysis and satellite data sets of ozone, methane and nitrous oxide. While it is difficult to generate a QBO signal internally in a global climate model, a model with the ability to simulate a QBO presents significant advantages in predicting the future evolution of the stratosphere: climate change is likely to modify the GWD, which will remotely modify stratospheric climate and variability. Capturing this feedback will require a modelled QBO forced

by an interactive GWD source spectrum, driven by changes in, for example, convective precipitation.

Acknowledgements. The authors thank NASA's MAP and ACMAP programmes for funding, S. M. Frith for processing the model output, and S. Strahan and three anonymous reviewers for their helpful feedback.

Edited by: M. Dameris

References

Andrews, A. E., Boering, K. A., Daube, B. C., Wofsy, S. C., Loewenstein, M., Jost, H., Podolske, J. R., Webster, C. R., Herman, R. L., Scott, D. C., Flesch, G. J., Moyer, E. J., Elkins, J. W., Dutton, G. S., Hurst, D. F., Moore, F. L., Ray, E. A., Romashkin, P. A., and Strahan S. E.: Mean ages of stratospheric air derived from in situ observations of CO_2, CH_4, and N_2O, J. Geophys. Res., 106, 295–314, 2001.

Baldwin, M. P., Gray, L. J., Dunkerton, T. J., Hamilton, K., Haynes, P. H., Randel, W. J., Holton, J. R., Alexander, M. J., Hirota, I., Horinouchi, T., Jones, D. B. A., Kinnersley, J. S., Marquardt, C., Sato, K., and Takahashi, M.: The quasi-biennial oscillation, Rev. Geophys., 39, 179–229, 2001.

Baldwin, M. P. and Dunkerton, T. J.: Quasi-biennial modulation of the southern hemisphere stratospheric polar vortex, Geophys. Res. Lett., 25, 3343–3346, 1998.

Butchart, N., Scaife, A. A., Austin, J., Hare, S. H. E., and Knight, J. R.: Quasi-biennial oscillation in ozone in a coupled chemistry-climate model, J. Geophys. Res., 108, D15, doi:10.1029/2002JD003004, 2003.

Douglass, A. R., Prather, M. J., Hall, T. M., Strahan, S. E., Rasch, P. J., Sparling, L. C., Coy, L., and Rodriguez, J. M.: Choosing meteorological input for the global modelling initiative assessment of high-speed aircraft, J. Geophys. Res., 104, 545–564, 1999.

Engel, A., Möbius, T., Bönisch, H., Schmidt, U., Heinz, R., Levin, I., Atlas, E., Aoki, S., Nakazawa, T., Sugawara, S., Moore, F., Hurst, D., Elkins, J., Schauffler, S., Andrews, A., and Boering, K.: Age of stratospheric air unchanged within uncertainties over the past 30 yr, Nat. Geosci., 2, 28–31, 2009.

Froidevaux, L., Jiang, Y. B., Lambert, A., Livesey, N. J., Read, W. G., Waters, J. W., Browell, E. V., Hair, J. W., Avery, M. A., McGee, T. J., Twigg, L. W., Sumnicht, G. K., Jucks, K. W., Margitan, J. J., Sen, B., Stachnik, R. A., Toon, G. C., Bernath, P. F., Boone, C. D., Walker, K. A., Filipiak, M. J., Harwood, R. S., Fuller, R. A., Manney, G. L., Schwartz, M. J., Daffer, W. H., Drouin, B. J., Cofield, R. E., Cuddy, D. T., Jarnot, R. F., Knosp, B. W., Perun, V. S., Snyder, W. V., Stek, P. C., Thurstans, R. P., and Wagner, P. A.: Validation of Aura Microwave Limb Sounder stratospheric and mesospheric ozone measurements, J. Geophys. Res., 113, D15S20, doi:10.1029/2007JD008771, 2008.

Garfinkel, C. I. and Hartmann, D. L.: Effects of the El Niño-Southern Oscillation and the Quasi-Biennial Oscillation on polar temperatures in the stratosphere, J. Geophys. Res., 112, D19112, doi:10.1029/2007JD008481, 2007.

Gray, L. J. and Pyle, J. A.: A two-dimensional model of the quasi-biennial oscillation of ozone, J. Atm. Sci., 46, 203–220, 1989.

Grooss, J.-U. and Russell III, James M.: Technical note: A stratospheric climatology for O_3, H_2O, CH_4, NO_x, HCl and HF derived from HALOE measurements, Atmos. Chem. Phys., 5, 2797–2807, doi:10.5194/acp-5-2797-2005, 2005.

Holton, J. R. and Lindzen, R. S.: An Updated Theory for the Quasi-Biennial Cycle of the Tropical Stratosphere, J. Atmos. Sci., 29, 1076–1080, doi:10.1175/1520-0469(1972)029<1076:AUTFTQ>2.0.CO;2, 1972.

Holton, J. R. and Tan, H.-C.: The Influence of the equatorial quasi-biennial oscillation on the global circulation at 50 mb, J. Geophys. Res., 37, 2200–2208, 1980.

Hurwitz, M. M., Newman, P. A., Li, F., Oman, L. D., Morgenstern, O., Braesicke, P., and Pyle, J. A.: Assessment of the Breakup of the Antarctic Polar Vortex in Two New Chemistry-Climate Models, J. Geophys. Res., 115, D07105, doi:10.1029/2009JD012788, 2010.

Hurwitz, M. M., Newman, P. A., Oman, L. D., and Molod, A. M.: Response of the Antarctic stratosphere to two types of El Niño events, J. Atmos. Sci., 68, 812–822, 2011a.

Hurwitz, M. M., Song, I.-S., Oman, L. D., Newman, P. A., Molod, A. M., Frith, S. M., and Nielsen, J. E.: Response of the Antarctic stratosphere to warm pool El Niño Events in the GEOS CCM, Atmos. Chem. Phys., 11, 9659–9669, doi:10.5194/acp-11-9659-2011, 2011b.

Jiang, Y. B., Froidevaux, L., Lambert, A., Livesey, N. J., Read, W. G., Waters, J. W., Bojkov, B., Leblanc, T., McDermid, I. S., Godin-Beekmann, S., Filipiak, M. J., Harwood, R. S., Fuller, R. A., Daffer, W. H., Drouin, B. J., Cofield, R. E., Cuddy, D. T., Jarnot, R. F., Knosp, B. W., Perun, V. S., Schwartz, M. J., Snyder, W. V., Stek, P. C., Thurstans, R. P., Wagner, P. A., Allaart, M., Andersen, S. B., Bodeker, G., Calpini, B., Claude, H., Coetzee, G., Davies, J., De Backer, H., Dier, H., Fujiwara, M., Johnson, B., Kelder, H., Leme, N. P., König-Langlo, G., Kyro, E., Laneve, G., Fook, L. S., Merrill, J., Morris, G.,Newchurch, M., Oltmans, S., Parrondos, M. C., Posny, F., Schmidlin, F.,Skrivankova, P., Stubi, R., Tarasick, D., Thompson, A., Thouret, V., Viatte, P., Vömel, von Der Gathen, H. P., Yela, M., and Zablocki, G.: Validation of the Aura Microwave Limb Sounder ozone by ozonesonde and lidar measurements, J. Geophys. Res., 112, D24S34, doi:10.1029/2007JD008776, 2007.

Lait, L. R., Schoeberl, M. R., and Newman, P. A.: Quasibiennial modulation of the Antarctic ozone depletion, J. Geophys. Res., 94, 559–571, 1989.

Lindzen, R. S. and Holton, J. R.: A Theory of the Quasi-Biennial Oscillation, J. Atmos. Sci., 25, 1095–1107, doi:10.1175/1520-0469(1968)025<1095:ATOTQB>2.0.CO;2, 1968.

Livesey, N. J., Filipiak, M. J., Froidevaux, L., Read, W. G., Lambert, A., Santee, M. L., Jiang, J. H., Pumphrey, H. C., Waters, J. W., Cofield, R. E., Cuddy, D. T., Daffer, W. H., Drouin, B. J., Fuller, R. A., Jarnot, R. F., Jiang, Y. B., Knosp, B. W., Li, Q. B., Perun, V. S., Schwartz, M. J., Snyder, W. V.,Stek, P. C., Thurstans, R. P., Wagner, P. A., Avery, M., Browell, E. V., Cammas, J.-P., Christensen, L. E., Diskin, G. S., Gao, R.-S., Jost, H.-J., Loewenstein, M., Lopez, J. D., Nedelec, P., Osterman, G. B., Sachse, G. W., and Webster, C. R.: Validation of Aura Microwave Limb Sounder O_3 and CO observations in the upper troposphere and lower stratosphere, J. Geophys. Res., 113, D15S02, doi:10.1029/2007JD008805, 2008.

Livesey, N. J., Read, W. G., Froidevaux, L., Lambert, A., Manney, G. L., Pumphrey, H. C., Santee, M. L., Schwartz, M. J.,Wang, S., Cofeld, R. E., Cuddy, D. T., Fuller, R. A., Jarnot, R. F., Jiang, J. H., Knosp, B. W., Stek, P. C., Wagner, P. A., and Wu, D. L.: Earth Observing System (EOS) Aura Microwave Limb Sounder (MLS) Version 3.3 Level 2 data quality and description document, JPL D-33509, 2011.

Lu, H., Baldwin, M. P., Gray, L. J., and Jarvis, M. J.: Decadal-scale changes in the effect of the QBO on the northern stratospheric polar vortex, J. Geophys. Res., 113, D10114, doi:10.1029/2007JD009647, 2008.

Molod, A., Takacs, L., Suarez, M., Bacmeister, J., Song, I.-S., and Eichmann, A.: The GEOS-5 Atmospheric General Circulation Model, Mean Climate and Development from MERRA to Fortuna, Technical Report Series on Global Modeling and Data Assimilation, Vol. 28., available at: http://gmao.gsfc.nasa.gov/pubs/docs/Molod484.pdf, 2012.

Newman, P. A., Nash, E. R., and Rosenfield, J. E.: What controls the temperature of the Arctic stratosphere during the spring?, J. Geophys. Res., 106, 19999–20010, doi:10.1029/2000JD000061, 2001.

Oman, L. D., Waugh, D. W., Kawa, S. R., Stolarski, R. S., Douglass, A. R., and Newman, P. A.: Mechanisms and feedback causing changes in upper stratospheric ozone in the 21st century, J. Geophys. Res., 115, D05303, doi:10.1029/2009JD012397, 2010.

Pawson, S., Stolarski, R. S., Douglass, A. R., Newman, P. A., Nielsen, J. E., Frith, S. M., and Gupta, M. L.: Goddard Earth Observing System chemistry-climate model simulations of stratospheric ozone-temperature coupling between 1950 and 2005, J. Geophys. Res., 113, D12103, doi:10.1029/2007JD009511, 2008.

Punge, H. J. and Giorgetta, M. A.: Net effect of the QBO in a chemistry climate model, Atmos. Chem. Phys., 8, 6505–6525, doi:10.5194/acp-8-6505-2008, 2008.

Randel, W. J. and Cobb, J. B.: Coherent variations of monthly mean total ozone and lower stratospheric temperature, J. Geophys. Res., 99, 5433–5447, 1994.

Rayner, N. A., Parker, D. E., Horton, E. B., Folland, C. K., Alexander, L. V., Rowell, D. P., and Kaplan, A.: Global analyses of sea surface temperature, sea ice, and night marine air temperature since the late nineteenth century, J. Geophys. Res., 108, 4407, doi:10.1029/2002JD002670, 2003.

Richter, J. H., Sassi, F., and Garcia, R. R.: Toward a physically based gravity wave source parameterization in a general circulation model, J. Atmos. Sci., 67, 136–156, 2010.

Rienecker, M. M., Suarez, M. J., Gelaro, R., Todling, R., Bacmeister, J., Liu, E., Bosilovich, M. G., Schubert, S. D., Takacs, L., Kim, G.-K., Bloom, S., Chen, J., Collins, D., Conaty, A., da Silva, A., Gu, W., Joiner, J., Koster, R. D., Lucchesi, R., Molod, A., Owens, T., Pawson, S., Pegion, P., Redder, C. R.,Reichle, R., Robertson, F. R., Ruddick, A. G., Sienkiewicz, M., and Woollen, J.: MERRA – NASA's Modern-Era Retrospective Analysis for Research and Applications, J. Climate, 24, 3624–3648, doi:10.1029/93JD00799, 2011.

Russell, J. M., Gordley, L. L., Park, J. H., Drayson, S. R., Tuck, A. F., Harries, J. E., Cicerone, R. J., Crutzen, P. J., and Frederick, J. E.: The halogen occultation experiment, J. Geophys. Res., 98, 10777–10797, 1993.

SPARC CCMVal: SPARC Report on the Evaluation of Chemistry-Climate Models, edited by: Eyring, V., Shepherd, T. G., and Waugh, D. W., SPARC Report No. 5, WCRP-132, WMO/TDNo. 1526, available at: http://www.atmosp.physics.utoronto.ca/SPARC, 2010.

Tian, W. S., Chipperfield, M. P., Gray, L. J., and Zawodny, J. M.: Quasi-biennial oscillation and tracer distributions in a coupled chemistry-climate model, J. Geophys. Res., 111, D20301, doi:10.1029/2005JD006871, 2006.